Modelling, Simulation and Control of a Fixed-Wing Unmanned Aerial Vehicle (UAV)

Conference Paper · December 2017

DOI: 10.26678/ABCM.COBEM2017.COB17-2703

Willian Rigon Silva
Universidade Federal de Santa Maria

Andre Luis da Silva
Universidade Federal de Santa Maria

24th COBEM - 2017

ABCM Associação Brasileira de Engenharia e Ciências Mecânicas

24th ABCM International Congress of Mechanical Engineering
December 3-8, 2017, Curitiba, PR, Brazil

COBEM-2017-2703
MODELLING, SIMULATION AND CONTROL OF FIXED-WING UNMANNED AERIAL VEHICLE (UAV)

Willian Rigon Silva
André Luís da Silva
UFSM - Grupo de Sistemas Aeroespaciais e Controle (GSAC) - RS, Brasil
willian.sky88@gmail.com
taurarm@gmail.com

Hilton Abílio Gründling
UFSM - Grupo de Eletrônica de Potência e Controle (GEPOC) - RS, Brasil
ghilton03@gmail.com

Abstract. *The work presents a methodology for mathematical modelling, simulation and control design for the longitudinal dynamics of a fixed-wing Unmanned Aerial Vehicle (UAV). The methodology used is well known in aeronautical literature for manned airplane design, so its adaptation to UAV was investigated. Due to the non-linear coupled dynamics present in this type of plant, some assumptions were made during the modelling and control design. Two models of the UAV were obtained: one purely analytic (by stability and control derivatives given by USAF DATCOM), and the other by X-Plane Flight Simulator (which uses Blade Element Theory to calculate the flight model). The analytical model was linearized for a chosen equilibrium point (cruise flight at chosen altitude and speed). The longitudinal flight dynamic modes were analysed: Short Period and Phugoid Mode. The chosen plant is the University of Toronto Explorer (UT-X) UAV, designed and built by the University of Toronto Aerospace Team (UTAT). Using classical automatic flight control theory, an Altitude and Mach Hold Autopilot was designed. A Software In The Loop (SITL) simulation was developed, using MATLAB/Simulink communicating with X-Plane through UDP protocol. The SITL simulation setup was used to perform virtual flight tests, in order to assess the performance of the designed autopilots. Wind, Gust and Turbulence tests were also presented.*

Keywords: *Flight Dynamics, Simulation, Autopilot, Control, UAV*

1. INTRODUCTION

The paper presents a methodology to model the longitudinal dynamics of an UAV by two methods: stability and control derivatives (given by USAF DATCOM), and virtual flight tests using X-Plane flight simulator.

The analytical model is composed by fixed-wing airplane equations of motion derived with Newtonian Mechanics, using Flat-Earth model, with dimensionless aerodynamic coefficients calculated by stability and control derivatives given by USAF DATCOM, (Siddiqui and Khushnood, 2009). The longitudinal dynamics modes, phugoid and short-period, given by the analytical simulation were compared with the results of virtual flight tests in the X-Plane simulator. If the longitudinal dynamics for both models are similar, then it is possible to use the analytical model to design the autopilot using control theory, and test its performance in a Software In The Loop (SITL) simulation with the X-Plane model. In order to refine the analytical model, wind tunnel data and real flight test data should be used. This methodology is well known in aeronautical industry and it is used for manned airplanes (Stevens and Lewis, 1992).

The study main objectives are to answer the two following problems: First, given an UAV with already defined airframe and physical characteristics (weight, moments of inertia, surface deflections, engine), how to obtain a longitudinal dynamics mathematical model; Second, knowing an UAV mathematical model, how to design an autopilot (Altitude Hold and Mach Hold) that can be implemented in low performance hardware (microcontrollers).

Nowadays, UAVs are ubiquitous aircraft which are used in several applications, such as: hobby, aerial photography, topography, Search And Rescue (SAR), and military (Austin, 2010). Quad-rotors and fixed-wing are the most common types of UAVs, flying under direct control of an operator or autonomously (assisted flight). The use of these flying robots in civilian and military roles is increasing, justified by the advantages that they present.

A more recent name definition for UAVs is Remotely Piloted Aircraft (RPA). Aeronautical legislation discussions (internationally and in Brazil) stated that these types of aircraft cannot fly unassisted. In other words, a fully autonomous flight can only occur if exists an operator with direct communication with the vehicle, that can take control immediately if necessary. The term RPA is more precise, describing this legislation requirement. In this paper the term UAV will be used along the text, but RPA is a synonym.

UAVs exists in several different weights and sizes, designed for a specific purpose and sometimes referred as drones. For professional applications (civilian or military), the increasing use of this type of aircraft is justified by its advantages over the manned aircraft. The main advantages are the low flight-hour and maintenance cost. For instance, UAV aerial reconnaissance missions can be of high risk and demanding, taking long time on air, even more than one day without landing. Using UAVs in this type of mission can minimize the risk to occur human error, since the operators are comfortable, safe, and can be changed while the aircraft is on flight (Austin, 2010). The use of UAVs also present advantages in radioactive environments, precision agriculture, and wildfires identification/combat. Therefore, it is important to fully understand the UAVs technology (design and operation) in order to develop optimized designs to specific applications (Beard and McLain, 2012).

An usual reconnaissance UAV (Figure 1) can be viewed as a system composed of several smaller sub-systems (Figure 2): Airframe, Engine, Electrical, Payload, Communications, Sensors and Actuators, Autopilot, and Ground Control Station (GCS). The detailing about each system is beyond the scope of this paper. The UAV and the GCS together forms an Unmanned Aerial System (UAS).

Figure 1. University of Toronto eXplorer (UT-X) UAV

1.1 Automatic Flight Control

All sub-systems are important, but the "brain" of an UAV is the Autopilot. Without the development of advanced and robust flight control techniques the operation of UAVs will be nearly impossible. In the majority of professional UAV missions, the aircraft flies beyond visual range and sometimes overseas. The pilot only have telemetry information from the internal sensors and a video image time delay. The Autopilot is the sub-system that controls the command surfaces of the UAV in order to maintain stable flight, flying through waypoints given by the navigation system. Usually the ground pilot does not fly the UAV directly with a joystick, instead it gives discrete informations, such as: Waypoints, Altitude, and Speed. A guidance and navigation system is necessary to translate the navigation information given by the pilot to the embedded autopilot. Therefore, the autopilot must guarantee stable flight, reject disturbance, and correctly fly through the waypoints.

The control laws inside the autopilot sub-system must be designed taking into account the flight dynamics of the aircraft. In other words, it is necessary to mathematically model the UAV flight dynamics in order to design the autopilot. The mathematical model of an aircraft has utilities beyond the design of an autopilot, it can be used also to test the aircraft in different flight phases, with different configurations, without constructing a prototype (which it is costly and very time consuming) (Stevens and Lewis, 1992). Ideally, a mathematical model of an aircraft should be used in conceptual design to achieve the maximum desired flight qualities, without any Stability Augmentation System (SAS) activated.

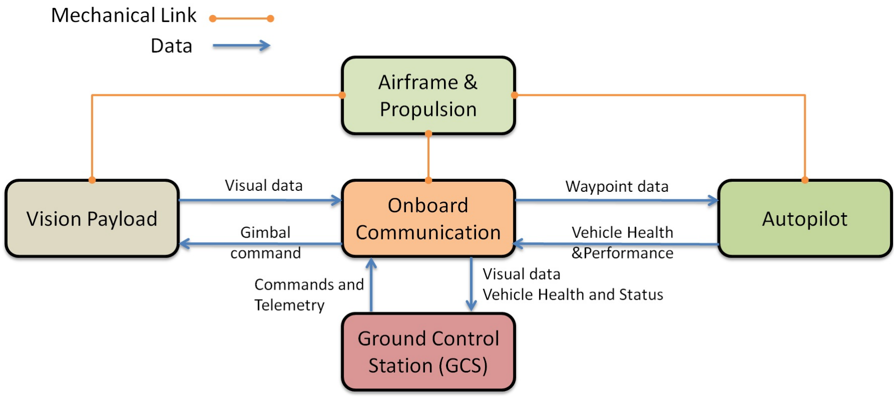

Figure 2. General reconnaissance UAV sub-systems, adapted from (UTAT, 2014)

2. PLANT - UT-X RECONNAISSANCE UAV

The UAV used in this study is the University of Toronto eXplorer (UTX) (Figure 1), designed and manufactured entirely by the University of Toronto Aerospace Team (UTAT), from Canada. One of the authors was an active member of UTAT, working on the Airframe, Payload, and Autopilot sub-systems. Former members of UTAT work as engineers at Bombardier and helped in the project. The UT-X was designed for aerial reconnaissance mission, focusing on two competitions: Unmanned Systems Canada Student UAV Competition (USC) and Association of Unmanned Vehicle Systems International (AUVSI) Student UAS Competition. The AUVSI competition is held in the Patuxent River Naval Air Station (NAS - Pax River), in MD, USA. This same NAS is the headquarters of the Naval Air Warfare Center Aircraft Division (NAWCAD), where the manned and unmanned aircraft prototypes are flight tested for the US NAVY. Therefore, currently the AUVSI competition is one of the most important UAS competitions in the world.

In a nutshell, the UT-X has pusher propeller/engine configuration with an electric motor, approximately 2 meters wingspan, with no sweep angle and dihedral angle of $4.1°$ (to increase natural roll stability), fixed tricycle landing gear, double vertical stabilizer tail, and horizontal stabilizer above propeller downwash. It has elevator, aileron, rudder, and throttle commands. Does not have slats or flaps. Its airframe is build in carbon fiber and kevlar stripes. The payload is a 29MP IMPERX high resolution camera (1.4Kg) and a Odroid computer to process the images before sending through a 5.8Ghz transmitter. The embedded autopilot is a 3DR PixHawk, sending telemetry data through a 900MHz transceiver and receiving commands through a 433MHz receiver.

One important characteristic to know, in order to do an analytical flight simulation, is the pitch moment of inertia. This characteristic is difficult to measure experimentally, specially for big aircraft. The method used in this study was to model all the UTX parts in a CAD software, such as SolidWorks, with the estimate weight and density of each part (wings, landing gear, payload, fuel/batteries, engine, etc). The SolidWorks uses a finite elements method to calculate the assembly moments of inertia, based on the weight and distribution of each part. This method is also used by (Parikh *et al.*, 2009).

The UTX technical characteristics are resumed in the Table 1. X_{cg} has positive values from the UAV's nose to its tail; Z_{cg} has positive values from down to up, starting from the UAV's belly.

3. MODELLING THE FLIGHT DYNAMICS

This section presents the considerations and procedures to obtain the longitudinal dynamics model of the UT-X. The construction of a mathematical model that describes the flight dynamics of an aircraft should be done in a very detailed way. The presented methodology is valid for the majority of fixed-wing airplanes, but its use in small/lightweight UAV is being investigated. An airplane generally posses 6 Degrees-of-Freedom (DoF) motion, with non-linear behavior. The flight of an airplane can be modeled by non-linear coupled differential equations, taking into account the forces and moments acting on it (Hull, 2007). It is desired that the mathematical model of an airplane (or UAV) is the simplest possible, yet precise and describing the reality (Stevens and Lewis, 1992). The process to build a mathematical model it is also iterative. Data from CFD simulations, wind-tunnel test and real flight test can refine the mathematical model (Stevens and Lewis, 1992).

To obtain such model, one can reproduce the following steps: Define a set of reference systems; Describe the translational (sum of forces) and rotational (sum of moments) motions using Newton's Second Law; Make considerations in order to simplify the equations of motion, decoupling the longitudinal and lateral-directional dynamics; Chose the state variables; Apply frame rotations in order to obtain the flight dynamics equations in the desired frame of reference; Linearize the model around an equilibrium point (choosing a specific speed and altitude); Obtain the stability and control derivatives using USAF DATCOM (or any other software), CFD simulations, Wind-Tunnel test, virtual flight tests, or real

Table 1. Physical Parameters of the UT-X UAV

Symbol	Parameter	Value
m	Total Mass with Payload and Batteries	$9.57\ kg$
$-$	Approximate Flight Autonomy	$45\ min$
V_{Tmax}	Approximate Maximum True Airspeed (TAS)	$25\ m/s$
b	Wingspan	$1.978\ m$
d	Body Length	$1.34\ m$
S	Wing Reference Area	$0.485\ m^2$
Λ	Wing Sweep Angle	$0.0\ °$
Γ	Wing Dihedral Angle	$4.1\ °$
I_{yy}	Pitch Moment of Inertia	$3.33\ kg.m^2$
$\bar{c}$	Aerodynamic Mean Chord	$0.2449\ m$
X_{cg}	Gravity Center Position at X axis	$0.477\ m$
Z_{cg}	Gravity Center Position at Z axis	$0.109\ m$
$W_{airfoil}$	Wing Airfoil	$NACA - 6412$
$HV_{airfoil}$	Horizontal and Vertical Stabilizers Airfoils	$NACA - 0012$

flight tests; Calculate the aerodynamic forces using the stability and control derivatives.

3.1 Considerations and Definition of Reference Frames

In order to simplify the model, some considerations should be done. By doing assumptions, we are allowing some errors that will be translated into limitations of this mathematical model. The errors of the model should be minimized, but we can incorporate the residual errors into the control system design. It is important to understand the model limitations, neglecting these limitations can lead to design error (that could be fatal).

The considerations done in order to obtain the longitudinal dynamics mathematical model, balancing simplicity and precision, are the following: The aircraft is in cruise flight phase; The atmosphere is stationary. The atmospheric properties only depends on altitude (i.e. they are independent of temperature variations and wind); The Earth surface is considered flat (Flat Earth Model), with no acceleration, no rotation, no translation, and with constant gravity intensity and direction (perpendicular to the Earth's surface); The aircraft body is considered rigid (rigid-body model) and with constant mass (mass is not a time function); The Sideslip angle (β) is zero; The perturbations around the equilibrium point are small (small pitch angles θ around trim point); The elevator deflection does not change forces, only the pitch moment; All aerodynamic forces (Lift,Drag,Thrust) act in the aircraft center of gravity (CG); The aircraft presents airframe symmetry in the x and z planes.

The forces and moments that act on an aircraft are produced by the relative wind passing through the aerodynamic surfaces (wings, body, command surfaces, and propulsive force). To determine the orientation and direction of these forces, it is necessary to define a system of reference. The equations of motion should be derived in relation to an inertial reference frame (RF) (Stevens and Lewis, 1992). Three reference frames (RFs) are defined (Figure 3):

(a) *Body Axes* - RF with 3 orthogonal axes, fixed on the aircraft CG. By convention, starting at the airplane CG, the X axis is pointing to airplane's nose, Y axis pointing to airplane's right wing, and Z axis pointing to airplane's bottom;

(b) *Stability Axes* - This RF is also known as North-East-Down(NED) frame. It has 3 orthogonal axes located at the airplane CG, with the X axis pointing North, Y axis pointing East, and Z axis pointing down (to the Earth's center);

(c) *Wind Axes* - RF with 3 orthogonal axes, fixed on the aircraft CG. These axes always follow the relative wind direction, with respect to the airplane. The X axis points in the reverse direction of the relative wind. The Z axis is perpendicular with the relative wind and it points down. The Y axis completes the system.

The inertial referential is chosen to be a fixed point in the Earth's surface. Even if the Earth has rotation and acceleration, they can be neglected since the time constants are different. The Earth acceleration is considerably slower than the acceleration of an aircraft maneuvering in its surface (Stevens and Lewis, 1992). Therefore, an inertial referential frame is fixed in the ground:

- *Ground Axes System* - RF with 3 orthogonal axes, fixed on the ground. The X and Y axes are parallel to the Earth's horizon (Flat Earth Model). It uses the NED convention.

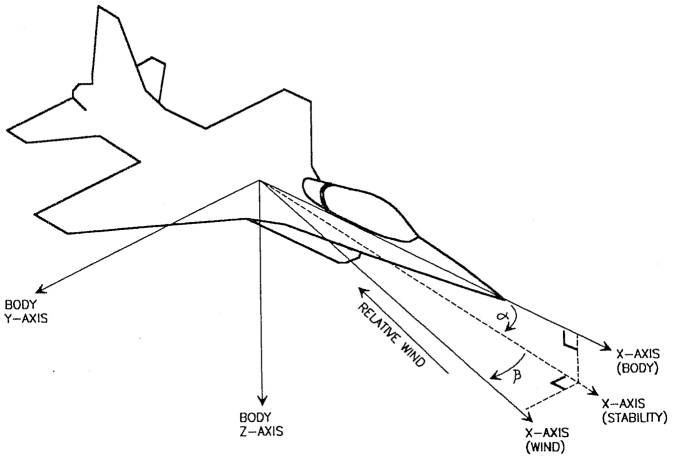

Figure 3. Airplane Reference Frames (Stevens and Lewis, 1992)

3.2 Non Linear Longitudinal Dynamics Model

To get a set of Longitudinal Dynamics equations in the desired RF, several steps should be made: Derive the forces and moments acting on the aircraft with respect to the inertial referential (using Newton's second law); Use rotation matrices (translating forces and moments from one RF to other); Calculate the aerodynamic forces with the stability and control derivatives (Lift, Drag, Thrust, Weight). The detailed development of the equations are presented in (Stevens and Lewis, 1992).

Since the model objective is to analyze the longitudinal dynamics modes (phugoid and short period) and design an autopilot, it is desired to get an state space model of the form (Eq. 1): $\mathbf{A}, \mathbf{B}, \mathbf{C}, \mathbf{D}$ are system parameters matrices; $\mathbf{X}$ is the state vector; $\mathbf{U}$ is the system's input vector; $\mathbf{Y}$ is the system's output vector.

$$\begin{aligned} \dot{\mathbf{X}} &= \mathbf{A}.\mathbf{X} + \mathbf{B}.\mathbf{U} \\ \mathbf{Y} &= \mathbf{C}.\mathbf{X} + \mathbf{D}.\mathbf{U} \end{aligned} \tag{1}$$

Using the considerations done in section 3.1 it is possible to decouple the longitudinal and lateral-directional dynamics. With this step, a non-linear longitudinal state space model is defined. The detailed development can be verified at (Stevens and Lewis, 1992), (Hull, 2007), and (Blakelock, 1991). A set of state variables and input variables is chosen, in reference to the inertial RF (Eq. 2). To get this set of variables, a series of frame rotations and variables substitutions is done.

$$\mathbf{X^T} = \begin{bmatrix} V_T & \alpha & \theta & Q & h \end{bmatrix} \quad ; \quad \mathbf{U^T} = \begin{bmatrix} \delta_e & \delta\pi \end{bmatrix} \tag{2}$$

Being: V_T is the airplane speed in relation to the relative wind; α is the Angle of Attack (AoA); θ is the pitch angle; Q is the pitch angular speed; h is the altitude; δ_e is the elevator deflection angle; δ_π is the engine throttle position (from 0 to 1).

The set of non linear differential equations using these state and input variables is defined by expanding the aerodynamic and propulsion forces, the moments of inertia, and the stability and control derivatives (Stevens and Lewis, 1992). This set is the representation of the longitudinal flight dynamics (Eq. 3):

$$\dot{V_T} = [\frac{(T.cos(\alpha) - D)}{m}] - g.sen(\gamma) \tag{3a}$$

$$\dot{\alpha} = \frac{[-T.sen(\alpha) - L + m.(V_T.Q + g.cos(\gamma))]}{(m.V_T + \bar{q}.S.C_{L\dot{\alpha}})} \tag{3b}$$

$$\dot{\theta} = Q \tag{3c}$$

$$\dot{Q} = \frac{(\bar{q}.S.\bar{c}.(C_M + K) + T.Z_E)}{I_{yy}} \tag{3d}$$

$$\dot{h} = V_T.sen(\gamma) \tag{3e}$$

$$\text{being} : K = \frac{[\frac{1}{2}.\bar{c}.(C_{MQ}.Q + C_{M\dot{\alpha}}.\dot{\alpha})]}{V_T} \tag{3f}$$

Where: $\gamma = \theta - \alpha$; g the acceleration due to gravity; m the mass of the airplane; L and D the aerodynamic forces of Lift and Drag respectively; T the propulsion force (Thrust); Z_E the offset of the propulsion axis z in relation to the airplane CG, in the UT-X case it is supposed to be zero; $\bar{q} = (1/2)\rho V_T^2$ the dynamic pressure (ρ is the air density); S the wing reference area; $\bar{c}$ the mean aerodynamic chord of the wing; $C_{L\dot{\alpha}}, C_{MQ}, C_{M\dot{\alpha}}$ are stability derivatives and C_M the pitch moment coefficient.

3.3 Aerodynamic Forces, Propulsion, and Stability and Control Derivatives

In order to calculate the aerodynamic forces (Eq. 4), it is needed to define the dimensionless aerodynamic coefficients. These coefficients are formed by stability and control derivatives, as a sum of one main influential part (usually depending on α and β angles) and several others of less influence (Stevens and Lewis, 1992) (Eq. 4). The stability derivatives are those considering the command surfaces in neutral position, the control derivatives are those referred to the changes in the command surfaces (e.g. δ_e).

$$L = \bar{q}.S.C_L, \tag{4a}$$
$$D = \bar{q}.S.C_D, \tag{4b}$$
$$C_L = C_{L0} + C_{L\alpha}\alpha \tag{4c}$$
$$C_D = C_{D0} + C_{DC_L}C_L^2 \tag{4d}$$
$$C_M = C_{M0} + C_{M\alpha}\alpha + C_{M\delta_e}\delta_e; \tag{4e}$$

Being: $T_C = \frac{T}{\bar{q}.S_D}$ - Is the normalized dimensionless propulsive coefficient, being the part that considerate the air pushed from the propeller to the wings; S_D is the propeller disc area. The other terms are defined in table 2.

The propulsive force (Eq. 5) is modelled depending on the engine type (electric, piston, turbo-prop, jet, turbo-fan, etc.). It was considered a propeller efficiency of 70%, more engine parameters are shown at Table 2.

$$T = (T_S + V_T.\frac{dT}{dV}).\delta_\pi \tag{5}$$

T_S is the static thrust, at zero altitude and zero speed; $\dfrac{dT}{dV} = -\dfrac{T_S}{V_{Tmax}}$ - Thrust decrease rate in relation to speed.

The stability and control derivatives for the UTX UAV were obtained using USAF DATCOM (Siddiqui and Khushnood, 2009), which uses semi-empirical methods, wind-tunnel data, and real flight test data to calculate the derivatives. The input for DATCOM was a FORTRAN language program describing the UTX (geometry and physical characteristics), accordingly to DATCOM rules. The dimensionless derivatives given by DATCOM are shown in Table 2.

4. SIMULATION

The state model has 7 variables (Eq. 2), but only 5 equations (Eq. 3). Therefore, it is needed to chose the values for 2 variables in order to solve this set of non linear longitudinal equations (for derivatives equal zero). Since it is considered only the cruise flight phase, the speed (V_T) and altitude (h) are chosen. An equilibrium point (trim point) is calculated using MATLAB/Simulink software, finding the elevator deflection (δ_e) and throttle percentage (δ_π) necessary to fly in the desired speed and altitude. The δ_{eE} is a negative value, indicating the trailing edge going up (accordingly to (Stevens and Lewis, 1992) convention). The trim values are shown at Table 2.

Table 2. Simulation variables definition:

Symbol	Parameter	Value	Symbol	Parameter	Value
V_{TE}	True airspeed (trim)	$20.58\ m/s$	h_E	Altitude (trim)	$200\ m$
α_E	AoA (trim)	$3.5385\ °$	θ_E	Pitch angle (trim)	$3.5385\ °$
δ_{eE}	Elevator deflection (trim)	$-3.7721\ °$	$\delta_{\pi E}$	Throttle (trim)	$80.43\ \%$
C_{L0}	Lift coefficient at zero AoA	0.423	$C_{L\alpha}$	Lift curve slope	0.0910
C_{D0}	Drag coefficient at zero lift	0.0342	C_{DC_L}	Induced drag derivative	0.0473
C_{M0}	Pitch moment coef. at zero AoA	0.0032	C_{MQ}	Pitch moment stability derivative	-13.5275
$C_{M\alpha}$	Pitch moment stability derivative	-0.0202	$C_{M\dot{\alpha}}$	Pitch moment stability derivative	-5.8614
$C_{M\delta_e}$	Pitch moment control derivative	-0.0181	Q_E	Pitch rate (trim)	$0\ °/s$
dT/dV	Thrust decrease rate over speed	-2.1353	T_S	Static Thrust	$5.44.g\ N$

4.1 Longitudinal Modes and Simulation Results

The analytical flight simulation of the UTX was done in MATLAB/Simulink, starting from the trim point. Considering that the UTX project presents a stable flight characteristics, it should present two longitudinal dynamics oscillations modes: short period and phugoid (Stevens and Lewis, 1992)(Blakelock, 1991)(Cook, 2011). The simulation objective is to identify the modes characteristics, such as: oscillation damping factor and frequency. In order to measure these values, the command inputs are the following: Maintain $\delta_{\pi E}$ at fixed trim value; Apply a doublet signal in the δ_e. Blue lines in figure 4 present the results of MATLAB/Simulink simulation, the short period mode happens as soon as the doublet signal is applied, it showed a fast and strongly dampened oscillation (lasting 3 seconds), making the UTX AoA oscillate from -10° to 15°. The phugoid mode starts to happen together with the short period mode, it showed a low frequency and weak dampened oscillation, lasting about 60 seconds. It is related with the change of energy between speed (V_T) and altitude (h). The phugoid mode result confirmed that the UTX has a stable aerodynamic project.

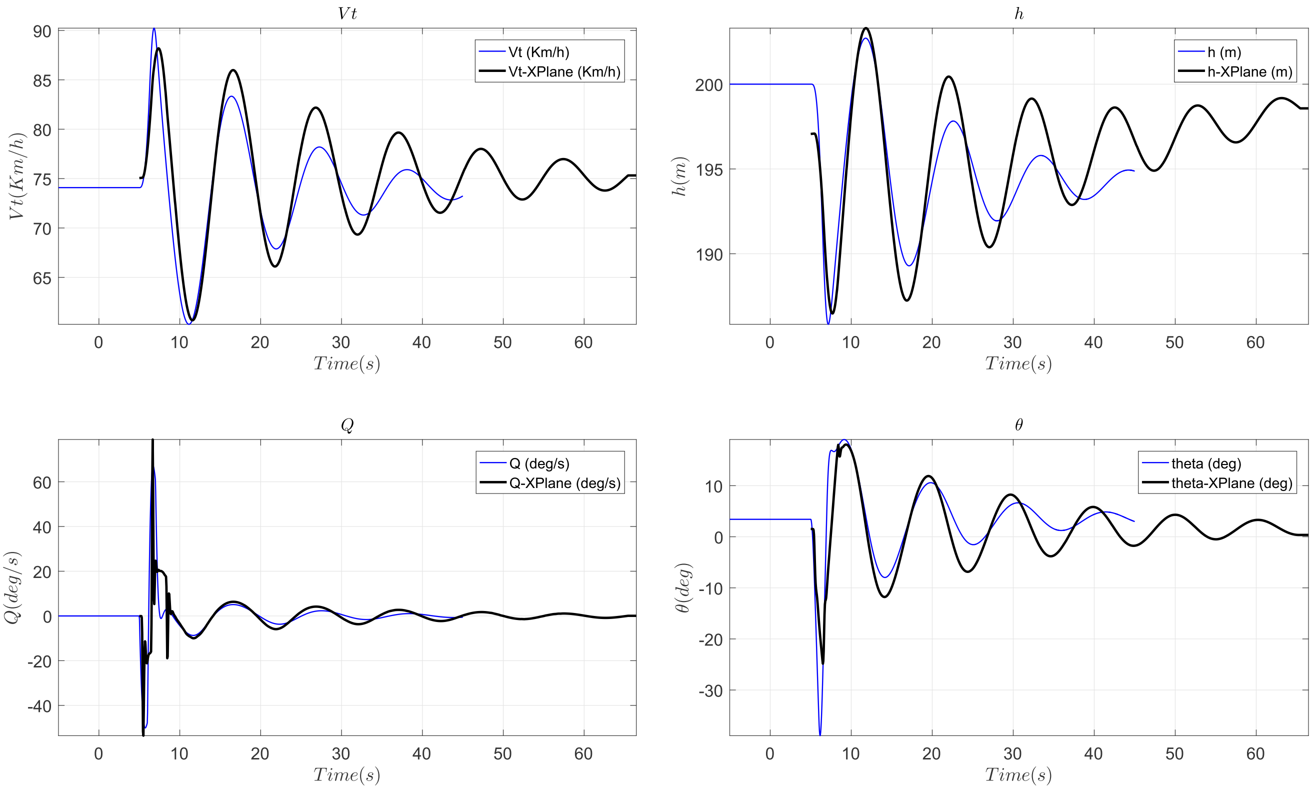

Figure 4. Comparison of analytical flight simulation and virtual flight simulation results

In order to compare the results of the analytical simulation, it is needed to get flight data of the same airplane with a different method (virtual test flight, wind-tunnel data or real test flight). Since at the time of this study a real test flight was not possible, a virtual flight test was performed at X-Plane flight simulator. The X-Plane was chosen because it calculates the aircraft model by using a different method of the stability and control derivatives. It uses a finite elements method to calculate the aerodynamic forces (Lift, Drag, Thurst) of each small part of the aircraft, at each time step of the simulation, this method is known as Blade Element Theory. X-Plane is also used for certified flight simulations (FAA-regulations), and have been used in several other flight dynamics and control studies (Figueiredo and Saotome, 2012)(Bittar *et al.*, 2013)(Thong, 2010). Therefore, a UTX model was designed inside X-Plane's Plane Maker software, the airfoils aerodynamic coefficients where obtained in JavaFoil software. With the UTX model built inside X-Plane environment, a virtual test flight was performed, flying the UTX to the desired trim altitude and applying the same type of doublet signal in δ_e manually, using a joystick. In other words, the virtual test flight repeated the same procedures of the analytical test flight. The results are shown in the red line of figure 4. It can be seen that the MATLAB/Simulink and X-Plane results are coherent. The best compatibility happens with the short period response. The X-Plane curves have a poorer behaviour, mainly because the manual command. Other major cause of incoherence is the engine model in X-Plane, that is most related to the long period response. In X-Plane, the engine model is more suitable for large airplanes.

In general, both modelling methods are approximated, but, the similar results indicate that both are reasonable for a preliminary analysis and design.

5. AUTOPILOT DESIGN

The controllers were designed using classical control techniques, also used in the aeronautical industry for manned airplanes (Stevens and Lewis, 1992). In order to design the flight control, the analytical model was linearized around the trim point (using the Jacobian matrix). The eigenvalues of the UTX UAV are shown in Eq. 6. Although the eigenvalues show that the UTX is an asymptotically stable system, it has a pole almost at the origin (turning into a marginally stable system). Analyzing the eigenvalues, it can be concluded that the short period mode dampening factor is 0.616 with frequency of $3.67 rad/s$. The phugoid mode dampening factor is 0.130 with frequency of $0.595 rad/s$. The controllers are designed in layers, with the most internal layer being the Stability Augmentation System (SAS), and the outermost layer being the Mach Hold Autopilot. The inner layers form an augmented state space system for the outer layers. This technique works because the the internal feedback variables have faster dynamics than the outer ones (different time constants).

$$\begin{Bmatrix} -2.2614 \pm 2.8899i \\ -0.0772 \pm 0.5898i \\ -0.0004 + 0.0000i \end{Bmatrix} \tag{6}$$

5.1 Stability Augmentation System (SAS)

The first control loop is the SAS, done with the feedback of the pitch rate (Q) (Figure 5). The main objective of SAS is to satisfy a frequency or dampening requirement for the short-period mode (Stevens and Lewis, 1992). It helps the airplane to become more stable, rejecting fast changes in pitch rate (e.g. that can be caused by wind-gust). The SAS controller gain is $K_q = -0.2$.

5.2 Controllability Augmentation System (CAS)

The second control loop is the CAS, with feedback of pitch angle (θ) (Figure 5). The main objective is to follow a reference for θ, this can be viewed as a Fly-By-Wire layer since the reference can be given by the pilot (in the joystick) or by the autopilot (numerically). However, a CAS can take different forms accordingly to its objectives (follow an AoA reference for instance). The CAS controller gain is $K_\theta = -0.8$.

5.3 Altitude Hold Autopilot

The third control layer is an Altitude HOLD Autopilot, which takes the feedback of altitude (h) (Figure 5). As the name says, the main objective is to follow an altitude reference, giving pitch angle reference input to the CAS controller. The altitude hold autopilot is a Proportional-Integrative (PI) type of controller: $PI_h(s) = -0.0002.(1 + 100.s)/s$

5.4 Mach Hold Autopilot (AutoThrottle)

The last control layer is an Mach Hold Autopilot, also known as AutoThrottle. This controller is not indicated in the figure 5. Its main objective is to maintain a desired speed by measuring it (feedback) and acting on the throttle percentage. The main difficulty to design such controller together with an altitude autopilot is because it is needed to take into account the augmented system created by closing the SAS, CAS and Altitude autopilot loops. To calculate the augmented system it was used state space model and matrix algebra. The Mach Hold autopilot is also of PI type: $PI_{V_T}(s) = -0.04.(1 + 50.s)/s$

5.5 Software In The Loop (SITL) Simulation Flight Test Results

To refine and assess the autopilot, a SITL simulation was performed using MATLAB/Simulink communicating via UDP protocol with X-Plane flight simulator. This SITL is possible because the analytical model is with accordance with the X-Plane model (as showed in previous section). In the SITL virtual test flight, the UTX altitude and speed were entirely controlled by the autopilot since take-off until landing. Even though the autopilot was designed only to the desired trim point, it also performs well out of this scope. Several tests were performed with constant wind, wind-gust, and turbulence, showing that the autopilot performed well in these conditions. A 10 minutes flight result can be viewed in Figure 6, from 300 to 430s of simulation there is wind-gusts, and from 380 to 430s there is presence of turbulence. A video showing the entire SITL can be viewed at Youtube's platform, on the internet (can be found searching for "uav willian" keywords or directly at www.youtube.com/watch?v=blhMO1KRQMU).

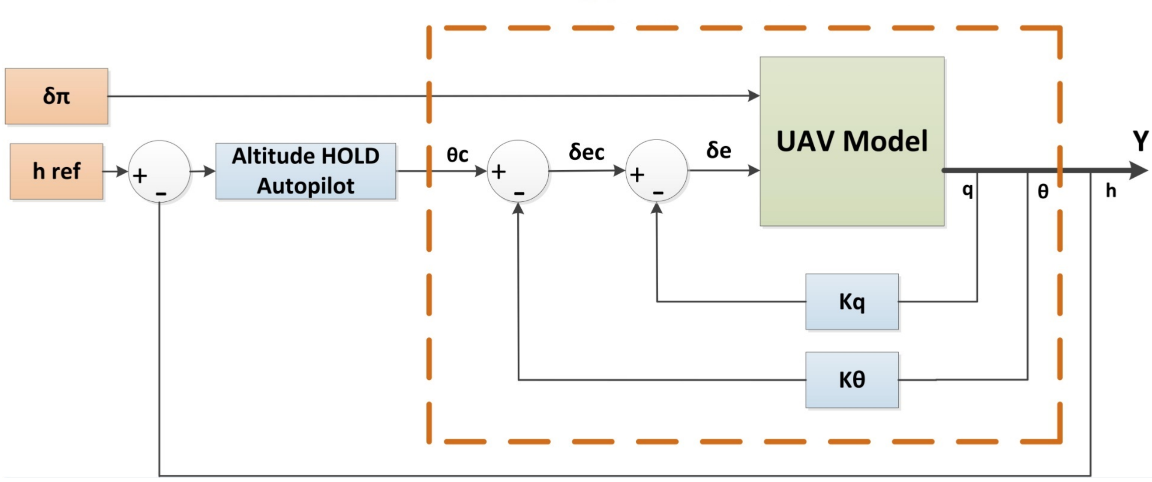

Figure 5. SAS,CAS, and Altitude Hold Autopilot control loops

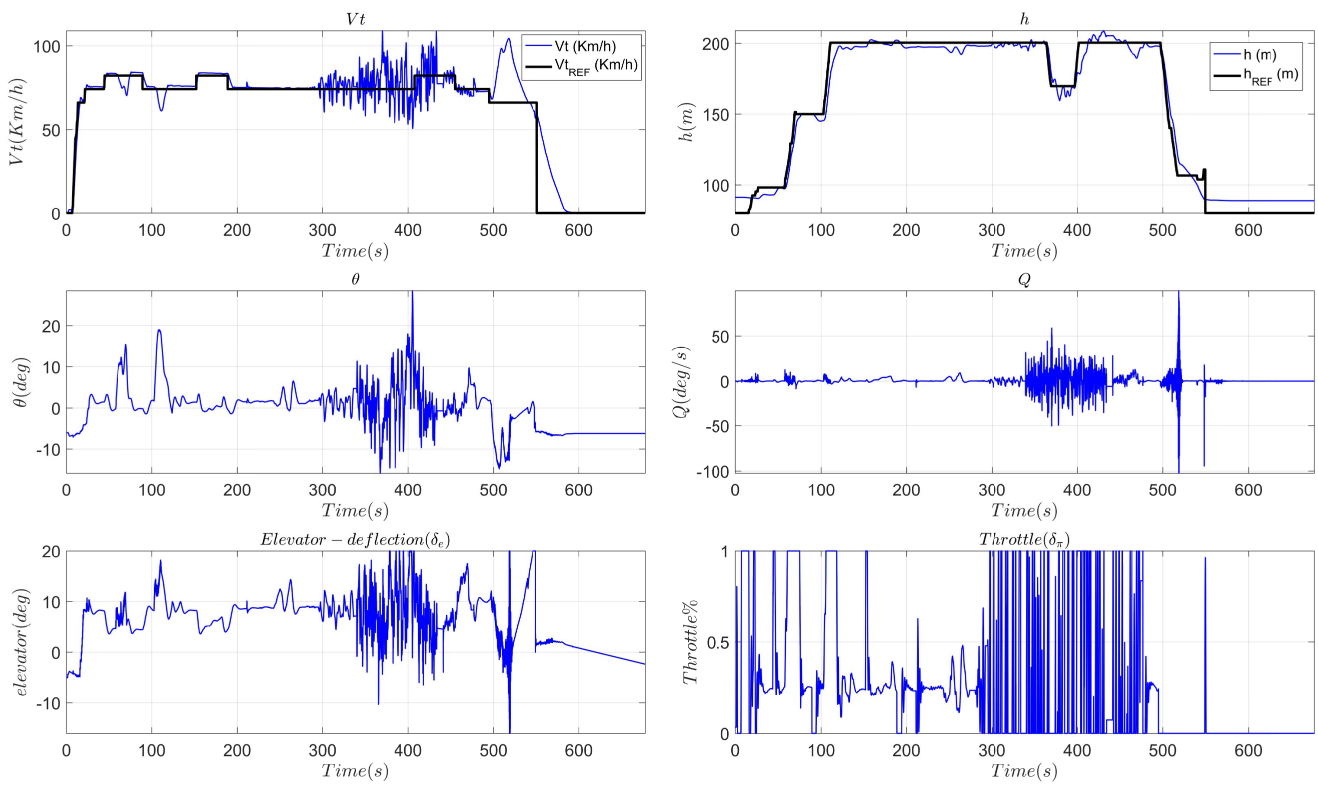

Figure 6. UTX SITL test flight results, from take-off to landing

6. CONCLUSION

The comparison of analytical (DATCOM-MATLAB/Simulink) with finite elements (X-Plane) models showed that both techniques presented similar responses for the UTX UAV. This result shows that this analysis methodology is interesting for simulating conceptual and real airplanes. The final data comparison should be made with real test flight data, to refine both analytical and X-Plane models. A refined analytical model can be used for control design, determining several layers of control (Stability Augmentation System (SAS), Controllability Augmentation System (CAS), Fly-By-Wire and Autopilot). With a X-Plane refined model, the flight control laws can be evaluated in a flight simulation environment, where pilots can fly and assess the control modes, serving also as a pilot training platform. For autopilot assess, the X-Plane can be used for Software in the Loop (SITL) and Hardware in the Loop (HITL) simulations. HITL can test the real flight computers that will be embedded in the real aircraft afterwards, considerably cutting the costs and risks to develop and test new flight computers. These techniques can also improve the training of pilots and operators.

7. ACKNOWLEDGEMENTS

The authors want to thanks the CAPES for the financial support to present this paper.

The author Willian Rigon Silva was an active member of University of Toronto Aerospace Team (UTAT), while studying in the University of Toronto (UofT), participating in a scholarship program called Science Without Borders (SwB).

8. REFERENCES

Austin, R., 2010. *Unmanned Aircraft Systems: UAVS Design, Development and Deployment*. John Wiley and Sons Ltd. Aerospace Series. ISBN 9780470058190.

Beard, R. and McLain, T., 2012. *Small Unmanned Aircraft: Theory and Practice*. Princeton University Press. ISBN 9780691149219.

Bittar, A., de Oliveira, N.M.F. and Figueiredo, H.V., 2013. "Hardware-in-the-loop simulation with x-plane of attitude control of a suav exploring atmospheric conditions". *J Intell Robot Syst (2014) 73:271–287*.

Blakelock, J., 1991. *Automatic Control of Aircraft and Missiles*. A Wiley-Interscience publication. ISBN 9780471506515.

Cook, M., 2011. *Flight Dynamics Principles: A Linear Systems Approach to Aircraft Stability and Control*. Elsevier aerospace engineering series. ISBN 9780080550367.

Figueiredo, H.V. and Saotome, O., 2012. "Modelagem e simulação de veículo aéreo não tripulado (vant) do tipo quadricóptero usando o simulador x-plane e simulink". *Anais do XIX Congresso Brasileiro de Automática, CBA 2012*.

Hull, D.G., 2007. *Fundamentals of Airplane Flight Mechanics*. Springer. ISBN 103540465715.

Parikh, K.K., Dogan, A., Subbarao, K., Reyes, A. and Huff, B., 2009. "Cae tools for modeling inertia and aerodynamic properties of an r/c airplane". *AIAA Atmospheric Flight Mechanics Conference 10 - 13 August 2009, Chicago, Illinois*.

Siddiqui, B.A. and Khushnood, A., 2009. "Improving usaf datcom predictions of aircraft nonlinear aerodynamics". *Canadian Aeronautics and Space Institute AERO'09 Conference Aerodynamics Symposium*.

Stevens, B.L. and Lewis, F.L., 1992. *Aircraft Control and Simulation*. John Wiley and Sons Ltd. ISBN 0471613975.

Thong, C.W.S., 2010. "Modeling aircraft performance and stability on x-plane". *Final Thesis Report 2010, SEIT, UNSW@ADFA*.

UTAT, 2014. "University of toronto explorer design report".

9. RESPONSIBILITY NOTICE

The authors are the only responsible for the printed material included in this paper.